Scientific Research Publishing

Computational Water, Energy, and Environmental Engineering, 2026, 15(1), 15-35
https://www.scirp.org/journal/cweee
ISSN Online: 2168-1570
ISSN Print: 2168-1562

Flood Risk Assessment in Irrigated Banana Perimeters of Tambacounda, Senegal Using the FIGUSED Multi-Criteria GIS Approach

Ousseynou Badji[1*], Lamine Diop[1,2], Aminata Sarr[3], Ansoumana Bodian[4], Aliou Diop[5]

[1]Faculty of Agronomic Sciences, Aquaculture and Food Technology, Gaston Berger University, Saint-Louis, Senegal
[2]Laboratory of Biological, Agronomic and Food Sciences and Modelling of Complex Systems (LABAAM), Gaston Berger University, Saint-Louis, Senegal
[3]Renewable Energy and Energy Efficiency Laboratory, International Institute for Water and Environmental Engineering (2iE), Ouagadougou, Burkina Faso
[4]Leïdi Laboratory-Dynamics of Territories and Development, Gaston Berger University (UGB), Saint-Louis, Senegal
[5]SAT, Gaston Berger University (UGB), Saint-Louis, Senegal
Email: *badji.ousseynou2@ugb.edu.sn

How to cite this paper: Badji, O., Diop, L., Sarr, A., Bodian, A. and Diop, A. (2026) Flood Risk Assessment in Irrigated Banana Perimeters of Tambacounda, Senegal Using the FIGUSED Multi-Criteria GIS Approach. *Computational Water, Energy, and Environmental Engineering*, **15**, 15-35.
https://doi.org/10.4236/cweee.2026.151002

Received: December 1, 2025
Accepted: January 23, 2026
Published: January 26, 2026

Abstract

In a context of increasing climate variability, the irrigated banana perimeters of the Tambacounda region (Senegal) are increasingly exposed to flood risks. This study aims to map vulnerable areas through a multi-criteria approach integrated into a Geographic Information System (GIS). The method used relies on the FIGUSED model Kazakis *et al.* (2015), which combines seven key environmental parameters: flow accumulation, slope, elevation, distance to drainage network, geology, land use and precipitation. Each parameter was normalized and weighted according to its relative influence on flood dynamics using the Analytical Hierarchy Process (AHP). The thematic layers were then overlaid to produce a synthetic flood vulnerability map. The results indicate that 40.12% of the study area is classified as high risk, mainly in low-lying zones near drainage axes, while 39.91% corresponds to low-risk areas, located on moderate relief. This mapping constitutes a decision-support tool for agricultural resource management, risk reduction and climate change adaptation. It also provides a technical basis for guiding mitigation actions and resilience strategies in a Sahelian context exposed to recurrent flooding.

Keywords

Flood Risk Mapping, FIGUSED, Multi-Criteria Analysis, GIS, Tambacounda, Banana Perimeters, AHP, Senegal

1. Introduction

Floods are among the most recurrent and destructive natural hazards worldwide [1]-[4]. Their increasing frequency is explained by the rise in extreme rainfall events, land degradation, and the rapid expansion of urban areas in ecologically fragile environments. This phenomenon is particularly pronounced in tropical and subtropical regions, where rainfall regimes are highly contrasted and urbanization is often poorly regulated [5]. According to the World Bank, more than 1.4 billion people currently live in flood-prone zones, with a large proportion located in low-income countries where prevention capacities remain limited (World Bank, 2020).

This vulnerability is particularly marked in sub-Saharan Africa, where floods and droughts have accounted for more than four-fifths of natural disasters recorded during the 20th century [6] [7]. Several structural factors contribute to this situation: fragility of rural environments, progressive degradation of watersheds, and the strong dependence of households on agricultural systems [8]-[10]. In Sahelian regions, low soil infiltration capacity, the absence of adequate hydraulic infrastructure, and high hydrological variability further aggravate flood risks, with direct consequences on agricultural activities and food security. Senegal exemplifies this situation. While research often focuses on urban centers such as Dakar, Kaolack, and Saint-Louis, agricultural areas of the interior remain highly exposed to seasonal flooding and intense runoff events [2] [11].

The Tambacounda region constitutes a highly representative case. Traversed by the Gambia River and accounting for nearly 60% of national banana production, it is characterized by low-gradient plains, compacted soils, and hydromorphic zones prone to water stagnation [12] [13]. Flooding in this region results from the combination of seasonal river flooding, intense rainfall, low topographic gradients, rapid soil saturation, and the organization of the natural drainage network. Several studies demonstrate that parameters such as slope, elevation, flow accumulation, distance to drainage, geology, or land use play a key role in the spatial distribution of flood susceptibility in tropical agricultural environments [14]-[16]. Between 2003 and 2024, the region recorded several major events that submerged more than one thousand hectares of cropland and caused significant economic and social losses [12] [13].

In this context, flood-risk mapping appears as an essential tool for territorial planning and the development of adaptation strategies. The combined use of Geographic Information Systems and multi-criteria approaches allows the integration of various environmental parameters within a coherent analytical framework an approach particularly relevant in regions with limited hydrological data [8] [17]. Among these approaches, the FIGUSED method has gained increasing interest. It is based on seven physical parameters weighted using the Analytical Hierarchy Process (AHP), a technique widely applied in different geographical contexts and considered appropriate for tropical environments where data may be incomplete [8] [14] [18] [19].

The present study follows this line of research by identifying and mapping flood-risk zones in the irrigated banana perimeters of Tambacounda using the FIGUSED method integrated into a GIS environment. The selected parameters include flow accumulation, slope, elevation, distance to drainage network, geology, land use and precipitation, in accordance with recognized methodological frameworks [14] [15].

The objective is twofold: 1) to identify the most flood-prone agricultural zones, and 2) to provide an operational decision-support tool for producers, local authorities, and development stakeholders. Ultimately, this approach contributes to strengthening the resilience of irrigated agricultural systems facing climatic hazards in an increasingly vulnerable Sahelian context.

2. Materials and Methods

2.1. Presentation of the Study Area

The study area is located in the southeastern part of Senegal, mainly within the region of Tambacounda, covering an area of approximately 9546.9 km^2 [13]. It extends on both sides of the Gambia River, between latitudes 13.517˚ North and longitudes −12.995˚ West, and includes the municipalities of Missirah, Nétéboulou, Dialacoto and Tambacounda, with extensions toward the bordering zones of Vélingara (Kolda) [12] [13]. **Figure 1** shows the general geographic configuration of the area.

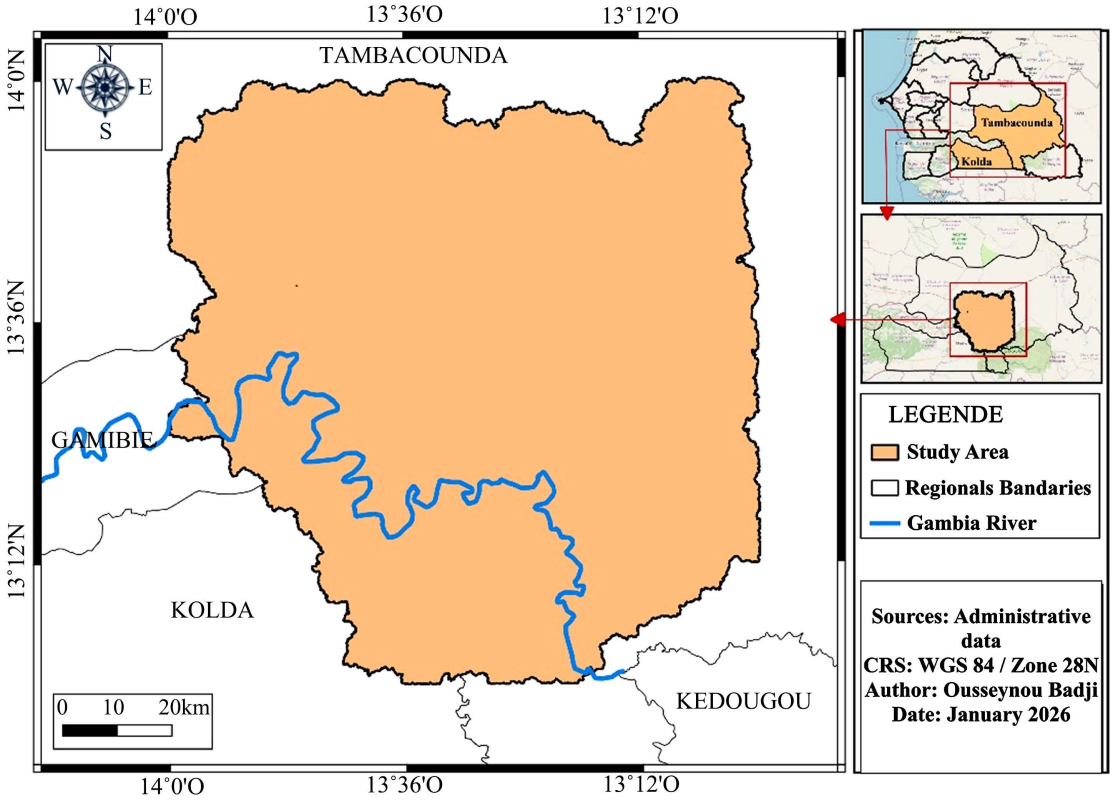

Figure 1. Location of the study area.

The climate is of the northern Sudanian type, characterized by a short and concentrated rainy season, with annual rainfall ranging between 568.8 mm and 1218 mm and an average temperature around 28.4˚C [12] [13].

The relief consists mainly of alluvial plains located between 10 and 20 m of elevation along the river, as well as weakly undulating plateaus reaching 30 to 60 m. These features shape the dynamics of runoff and flooding [13] [20]. Such geomorphological patterns, also observed in many tropical basins, are known to increase water concentration rates and flood frequency [16] [21].

The soils of the region are predominantly hydromorphic, rich in clay and organic matter, which gives them high water retention capacity. However, they are also subject to rapid saturation during intense rainfall events, increasing flood susceptibility [13] [20] [22].

The Gambia River constitutes the main water source for irrigation. Agricultural production relies on motor pumps and PVC canal networks, although equipment remains rudimentary and unevenly distributed across farms [13].

In the study area, more than 1000 hectares are devoted to banana cultivation, representing nearly 80% of national production. The sector is structured around economic interest groups (GIE) coordinated by APROVAG, which ensures organization and marketing of the harvests [12] [13]. Musa spp. plantations have progressively replaced natural savannas while maintaining interactions with neighboring ecosystems such as the Niokolo Koba National [12].

Historically, banana cultivation was introduced in the 1970s by OFADEC, with support from stakeholders such as USAID and Secours Catholique, before being taken over by local producers' organizations [12]. Since then, several major flood events particularly in 2003 and 2024 have submerged more than 1000 hectares and caused considerable material damage, confirming the persistent vulnerability of this agricultural zone [12] [13].

2.2. Flood Risk Index (IRBT)

A methodological approach based on recent research was applied to delineate the areas most exposed to flooding in the banana perimeters of Tambacounda. To achieve this, an index model was constructed and deployed within a GIS environment, with the main objective of identifying zones at risk of flooding. This model relies on a multi-criteria analysis integrating the Tambacounda Banana Plantation Risk Index (IRBT). This index allows the identification of critical flood-risk points and facilitates comparison between the different sub-basins in the region. The IRBT is a direct adaptation of the FIGUSED framework to the specific agro-hydrological conditions of the irrigated banana perimeters of Tambacounda. While it preserves the seven environmental parameters and the general structure of the FIGUSED model, the classification thresholds and some parameter definitions were adjusted to reflect local topography, land-use patterns and hydrological behaviour. The approach begins with the collection of relevant spatial data, processed using weighting methods, and leads to the production of a synthetic flood-risk map. A comparison with historical flood data is then performed to evaluate

the reliability of the method.

2.2.1. Collection of Relevant Spatial Data

The approach begins with the collection of spatial data required to formulate the IRBT. This index is constructed from seven key parameters: flow accumulation (F), precipitation intensity (I), geology (G), land use (U), slope (S), elevation (E), and distance to the hydrographic network (D), aggregated according to Equation (1):

$$\text{IRBT} = F + I + G + U + S + E + D \quad (1)$$

with:

- F: Flow accumulation
- I: Precipitation intensity
- G: Geology
- U: Land use (land cover)
- S: Slope
- E: Elevation
- D: Distance to the hydrographic network

Each parameter is standardized on a common scale ranging from 2 to 10, ensuring consistency between datasets.

The data used in this study originate from various complementary sources:

1) GPS survey points of the investigated farms, providing precise locations of banana plantations;

2) satellite data from SRTM and Sentinel-2, used to extract topographic, hydrological, and land-use information;

3) institutional databases, particularly from the National Agency of Civil Aviation and Meteorology (ANACIM), which provide essential historical and current climate data. A detailed description of data sources is presented in Table 1.

Table 1. Sources and methods of data collection.

Parameter (symbol)	Simplified Definition	Technical Description	Data Source/Origin	Access Link/Platform
Flow Accumulation (F)	Measures the amount of water that accumulates in an area.	Derived from the SRTM DEM using ArcGIS Flow Direction and Flow Accumulation tools. Identifies runoff convergence zones.	SRTM DEM (30 m), NGA/USGS	https://earthexplorer.usgs.gov/
Rainfall Intensity (I)	Evaluates the strength and frequency of rainfall.	Calculated using the Modified Fournier Index (MFI) based on rainfall data (1895-2023). Spatial interpolation (Spline method) in QGIS.	ANACIM (local weather stations)	https://www.anacim.sn
Geology (G)	Indicates soil type and its ability to absorb water.	Data extracted from the national geological map (DMGS). Clay soils (low permeability) are identified as more sensitive.	Base Geo Senegal	https://www.geosenegal.gouv.sn/

Continued

Land Use (*U*)	Type of land cover: crops, forests, urban areas, etc.	Processed using supervised classification of Sentinel-2 (2020) and Landsat 8 imagery. Specific identification of banana plantations.	Sentinel-2, Landsat 8	https://livingatlas.arcgis.com/landcoverexplorer/
Slope (*S*)	Terrain inclination. Flatter areas retain more water.	Calculated from the DEM in ArcGIS. Classified into five categories (<2.37% to very steep).	SRTM DEM (30 m), NGA	https://earthexplorer.usgs.gov/
Elevation (*E*)	Terrain altitude. Low-lying areas are more vulnerable.	Extracted directly from the SRTM DEM. Banana plantations between 50 - 90 m are particularly exposed.	SRTM DEM (30 m), NGA	https://earthexplorer.usgs.gov/
Distance to Hydrographic Network (*D*)	Distance between a point and the nearest watercourse.	Calculated using Stream Order from the DEM, then classified into buffer zones (<200 m to >2000 m). Higher risk near rivers.	SRTM DEM (30 m), NGA	https://earthexplorer.usgs.gov/

2.2.2. Weighting of Criteria and Weighted Formulation of the IRBT

The weighting of criteria was performed using the Analytical Hierarchy Process (AHP), a structured approach to rank interdependent factors based on their relative importance in flood dynamics. This method, validated through sensitivity tests, relies both on scientific literature [2] [14] and on the specific hydrological characteristics of Tambacounda.

Continuous variables such as elevation, flow accumulation, or rainfall intensity were classified into five classes according to geomorphological and hydrological progression, based on Demek (1972) and thresholds adapted to the region. Slope was categorized according to runoff behavior following Van Zuidam (1983). Qualitative criteria such as geology and land use were reclassified from national maps, Sentinel-2 land cover data, and field observations.

Each class was assigned a standardized score (generally 2 - 10) based on its influence on flood risk. A score r_i was assigned to each spatial cell for each criterion, then multiplied by a weight w_i defined by AHP, to compute the final index using the following formula [14]:

$$\begin{aligned} \text{IRBT} &= \sum_{i=1}^{7} r_i \cdot w_i \\ &= F \cdot w_f + I \cdot w_I + G \cdot w_G + U \cdot w_G + S \cdot w_S + E \cdot w_D + D \cdot w_D \end{aligned} \quad (2)$$

To determine these weights, a pairwise comparison matrix (**Table 1**) was constructed, in which each criterion was evaluated against the others using Saaty's scale (ranging from 1 to 9). The weighting assigned to each parameter was then normalized (**Table 2**) to ensure their comparability.

Table 2. Criteria comparison matrix (AHP).

Parameter	Flow Accum.	Drainage Dist.	Elevation	Land Use	Heavy Rainfall	Slope	Geology
Flow accumulation	1	2	2	3	3	5	7
Drainage distance	1/2	1	1	3	3	4	6
Elevation	1/2	1	1	3	3	4	6
Land use	1/3	1/3	1/3	1	2	4	5
Heavy rainfall	1/3	1/3	1/3	1/2	1	4	5
Slope	1/5	1/4	1/4	1/4	1/4	1	3
Geology	1/7	1/6	1/6	1/5	1/5	1/3	1

The high ranking of flow accumulation, elevation and distance to drainage is justified by the specific characteristics of the banana-growing plains of Tambacounda. The topography is extremely flat and the hydrographic network controls both runoff routing and stagnation, making small variations in elevation decisive for flood dynamics. Conversely, geology plays a minor role because the study area is dominated by relatively homogeneous lateritic and ferruginous substrates with limited contrasts in permeability.

The criteria weights obtained through the AHP process (**Table 3**) show that flow accumulation ($w = 3.0$) is the most influential factor, reflecting its central role in concentrating runoff in the low-gradient plains of Tambacounda. Distance to the drainage network and elevation ($w = 2.1$ each) constitute the second level of importance, since both strongly condition the accumulation and evacuation of surface water. Land use ($w = 1.2$) and rainfall intensity ($w = 1.0$) exert a moderate influence, while slope ($w = 0.5$) and geology ($w = 0.3$) display lower weights, consistent with the relatively homogeneous geomorphology and substrate of the study area.

Table 3. Standardized weightings of criteria.

Parameter	Flow Accum.	Drainage Dist.	Elevation	Land Use	Heavy Rainfall	Slope	Geology	Average	w_i (Weight)
Flow accumulation	0.33	0.39	0.39	0.27	0.24	0.22	0.21	0.30	3.0
Drainage distance	0.17	0.20	0.20	0.27	0.24	0.18	0.18	0.21	2.1
Elevation	0.17	0.20	0.20	0.27	0.24	0.18	0.18	0.21	2.1
Land use	0.11	0.07	0.07	0.09	0.16	0.18	0.15	0.12	1.2
Heavy rainfall	0.11	0.07	0.07	0.09	0.12	0.18	0.15	0.10	1.0
Slope	0.07	0.05	0.05	0.02	0.04	0.09	0.05	0.05	0.5
Geology	0.05	0.03	0.03	0.02	0.02	0.01	0.03	0.03	0.3

Based on these corrected weights, the final flood risk map was generated using a linear combination of the seven parameters following the FIGUSED methodology. Each factor (slope, elevation, land use, etc.) was normalized and multiplied by its respective AHP-derived weight to compute the final index. The weighted formulation of the IRBT is expressed as follows:

The final weighted equation of the IRBT index is formulated as follows:

$$\text{IRBT} = 1.2 \times F + 0.5 \times I + 0.4 \times G + 0.7 \times U + 1.6 \times S + 3.0 \times E + 2.5 \times D \quad (3)$$

This approach produces a continuous map of the risk index, whose values were subsequently classified into three hazard levels to facilitate interpretation:

- Low: IRBT ranging from 20.5 to 56.6 (blue)
- Moderate: IRBT ranging from 56.6 to 62.8 (yellow)
- High: IRBT ranging from 62.8 to 89.4 (red)

This interval-based classification allows for the visual identification of the most vulnerable areas according to their degree of susceptibility to flooding.

3. Results and Discussion

The analysis is based on a series of thematic maps developed from physical, climatic, and environmental parameters to characterize flood vulnerability within the banana-growing areas of Tambacounda. These information layers make it possible to spatialize risk factors in an integrated manner, consistent with approaches developed in hydrological assessments using GIS and multi-criteria methods [14] [23]-[26]. The methodology also aligns with studies that highlight the importance of combining topography, geology, land use, and rainfall to identify flood-prone areas [16] [21] [27]. However, it should be noted that although several of our results corroborate patterns observed in the literature, other studies conducted in different geographical contexts sometimes report contrasting or more nuanced hydrological behaviour.

3.1. Thematic Maps

3.1.1. Flow Accumulation (*F*)

The analysis shows that 54.05% of the area exhibits low flow accumulation, generally limiting the formation of floods. However, 46% of the surface displays moderate accumulation, suggesting localized risks, mainly in zones near drainage networks. The absence of areas with very high accumulation confirms the lack of extreme flood-prone sectors over large extents. Similar observations were reported in the NiériKo sub-basin, where accumulation patterns were concentrated in specific locations and strongly correlated with local morphology [2]. The effects of flow accumulation on flood generation are also documented in several tropical basins, where runoff is driven by flow direction and low slopes [16] [21]. However, some FIGUSED studies conducted in other environments show that flow accumulation may play a more or less important role depending on basin configuration. Kazakis *et al.* (2015) reported that in certain Mediterranean watersheds, accumulation is a secondary factor compared to elevation or distance to drainage,

which partially nuances our findings, where accumulation has an intermediate weight. The spatial distribution of these patterns is illustrated in Figure 2, which presents the flow accumulation index (*F*) across the basin.

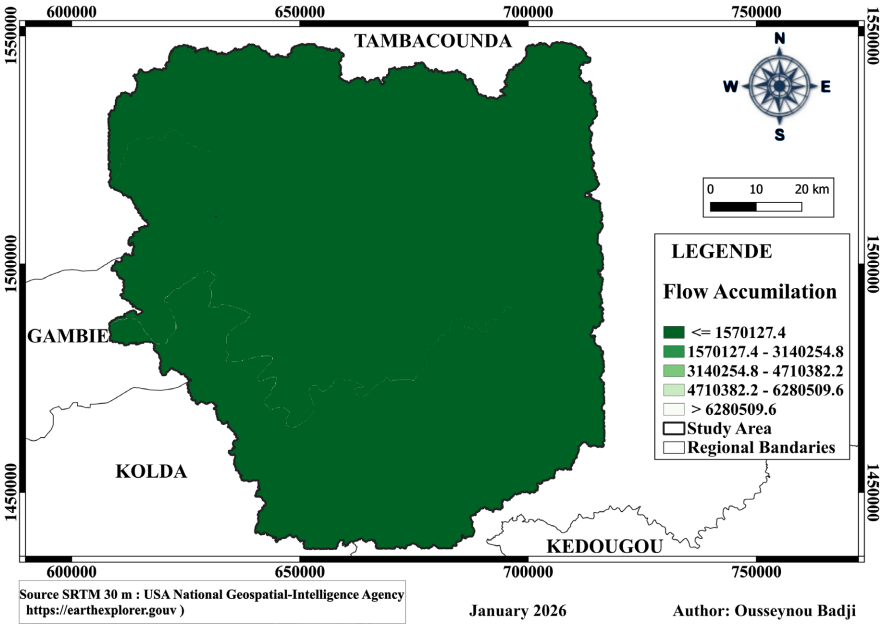

Figure 2. Flow accumulation index (F) in the basin.

3.1.2. Rainfall Intensity (*I*)

The results indicate that more than 55% of the area receives very high rainfall (>150 mm), which is a major determinant of flood occurrence, particularly in contexts of low slopes or compacted soils. Although some sectors receive low rainfall (38.67% ≤ 50 mm), the majority of the territory remains exposed to intense rainfall events. This pattern is consistent with results from the Kou basin in Burkina Faso, where zones with high rainfall (>1050 mm) showed strong flood susceptibility (Guelbeogo *et al.*, 2023). The relationship between extreme rainfall and rapid water rise is also described in other regional studies [25] [26]. Nevertheless, the literature does not fully converge on the weight of rainfall: in some FIGUSED applications, where rainfall variability is low, precipitation intensity appears only as a weakly determining factor [14]. This contrasts with our results, where pronounced spatial concentration of rainfall clearly increases vulnerability, underscoring the importance of local climatic context. The spatial distribution of these rainfall patterns is illustrated in Figure 3, which presents the precipitation intensity index (*I*) across the basin.

3.1.3. Geology (*G*)

The geological distribution is dominated by lateritic lithosols (40.88%), followed by poorly developed soils (25.57%) and tropical ferruginous soils (14.61%). Hydromorphic soils represent only 2.87% of the area. This composition indicates generally low permeability, promoting runoff and limiting infiltration during heavy rainfall events.

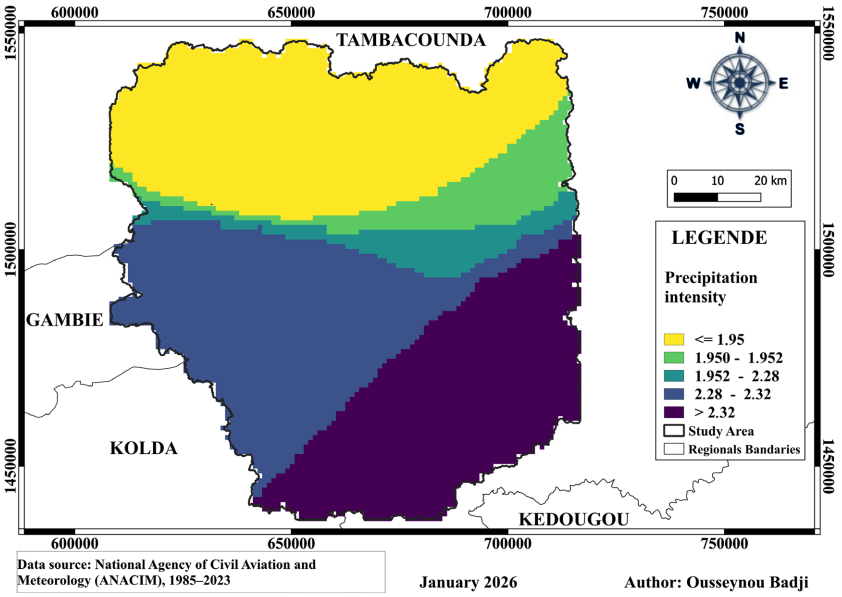

Figure 3. Precipitation intensity index (I) in the basin.

Similar characteristics have been reported in regions with impermeable substrates, where geology acts as an aggravating factor in flood formation [14]. The low infiltration capacity of lateritic crusts is also documented in several hydrological studies in West Africa [27]. However, some studies based on the FIGUSED method show that geology can sometimes be the least influential parameter in flood risk modeling, especially in basins with highly permeable substrate [14]. This suggests that although our study area presents low permeability favouring runoff, the relative importance of this factor can vary significantly from one region to another. The spatial expression of these geological patterns is illustrated in Figure 4, which presents the geology index (*G*) across the basin.

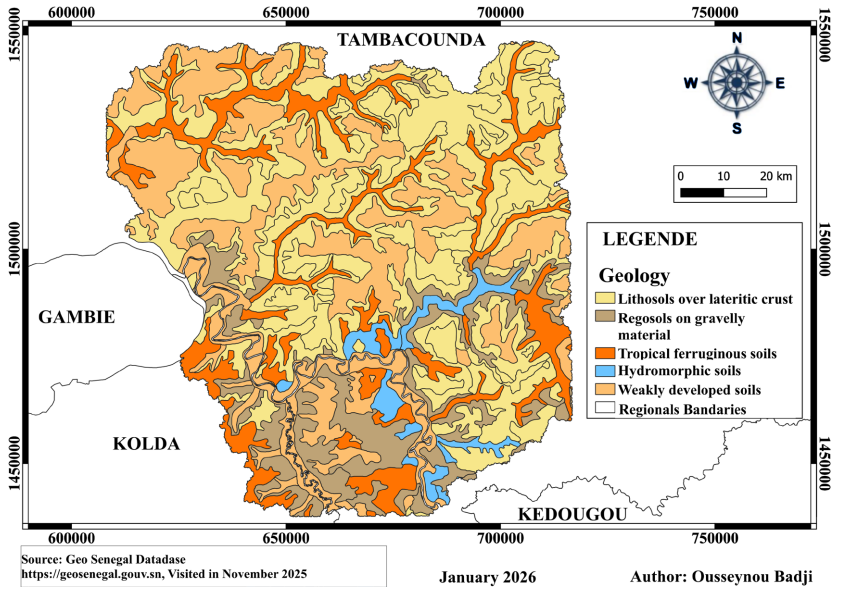

Figure 4. Geology index (G) in the basin.

3.1.4. Land Use (*U*)

The analysis reveals a strong predominance of bare soil (71%), which exposes the area to rapid runoff and low water retention. Vegetated zones (20.76%) and cultivated areas (7.46%) represent portions too limited to provide effective buffering.

This trend is consistent with findings from the Kou basin, where highly anthropized or degraded vegetation areas exhibited increased vulnerability to flooding [28]. The influence of vegetation loss on runoff dynamics is also supported by several hydrological studies using GIS [21] However, other studies indicate that the impact of land use may vary depending on the degree of human modification. In highly urbanized areas, LULC often becomes the dominant risk factor [29] whereas in agricultural or forested landscapes, it may become secondary to elevation or geology [14] These contrasts highlight that the role of LULC depends strongly on landscape structure. The spatial distribution of land use patterns is illustrated in **Figure 5**, which presents the land use index (*U*) across the basin.

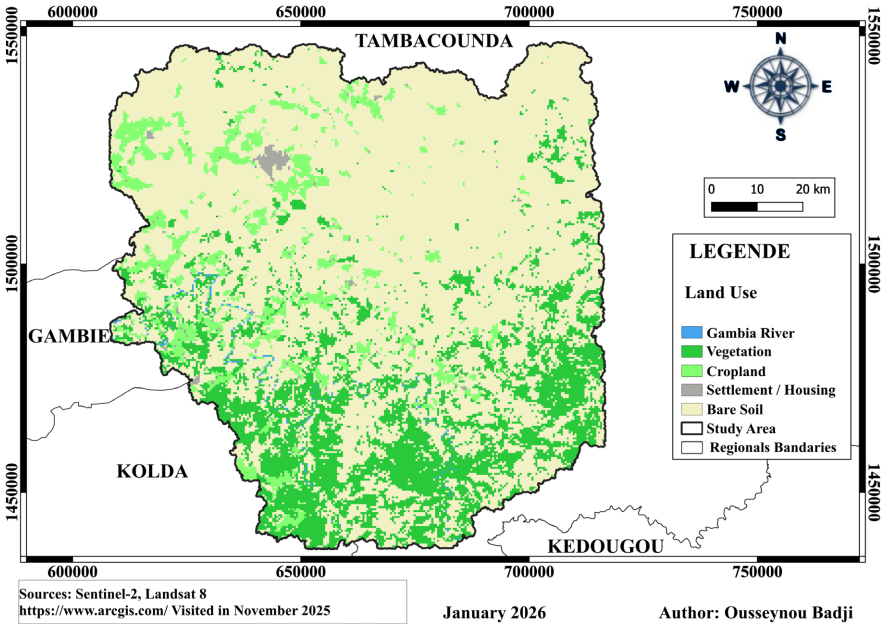

Figure 5. Land use index (U) in the basin.

3.1.5. Slope (*S*)

Gentle slopes (≤3.2˚) cover nearly 60% of the area, increasing the likelihood of water stagnation. Steeper slopes (41.64%) would favour better drainage, but remain a minority.

This configuration aligns with observations by C. Faye *et al.* (2021), which show that low-slope areas represent the most susceptible zones for water stagnation. The determining role of slope in flood occurrence is widely supported in hydrological literature [16] [21]. However, studies conducted in mountainous environments indicate that steep slopes can also favour rapid and violent flash floods [30], unlike our study area where low slopes increase waterlogging. This demonstrates that the effect of slope does not always act in the same direction depending on

geomorphological context. The spatial distribution of slope characteristics is illustrated in Figure 6, which presents the slope index (*S*) across the basin.

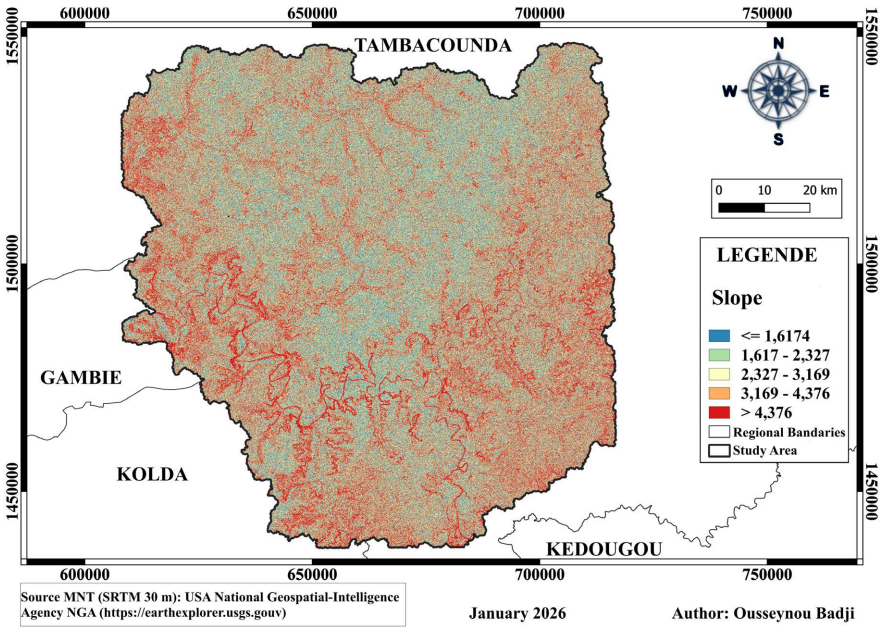

Figure 6. Slope index (S) in the basin.

3.1.6. Elevation (*E*)

More than 67% of the area lies between 42 and 78 m in altitude, indicating a generally low and homogeneous topography. Very low-lying zones (≤24 m) represent 9.19%, while elevations above 78 m are marginal (0.83%). Such configuration favours water stagnation, particularly during intense rainfall.

These findings are consistent with the FIGUSED model applied by Kazakis *et al.* (2015), which systematically identifies low-lying areas as highly flood-prone. Other studies confirm the direct link between low elevation and water concentration [26]. Nevertheless, in FIGUSED-S models, elevation is identified as the most determining factor in several regional studies [14], reinforcing our results while suggesting that its weight may be even higher elsewhere. Conversely, in mountainous landscapes, higher elevations may be the most exposed to torrential floods [31], contrasting with the relatively flat topography of our study area. The spatial distribution of elevation is illustrated in Figure 7, which presents the elevation index (*E*) across the basin.

3.1.7. Distance to Drainage Network (*D*)

The analysis shows that more than 60% of the area is located more than 1000 m away from natural outlets, limiting water evacuation and increasing flood risk. Only 20.85% of the area lies close to drainage networks (<500 m).

This result is consistent with observations by C. Faye *et al.* (2021), where areas far from outlets displayed high vulnerability. The importance of distance to drainage in flood susceptibility assessment is also emphasized in several multi-criteria GIS studies [16] [25]. However, some studies show that distance to drainage can

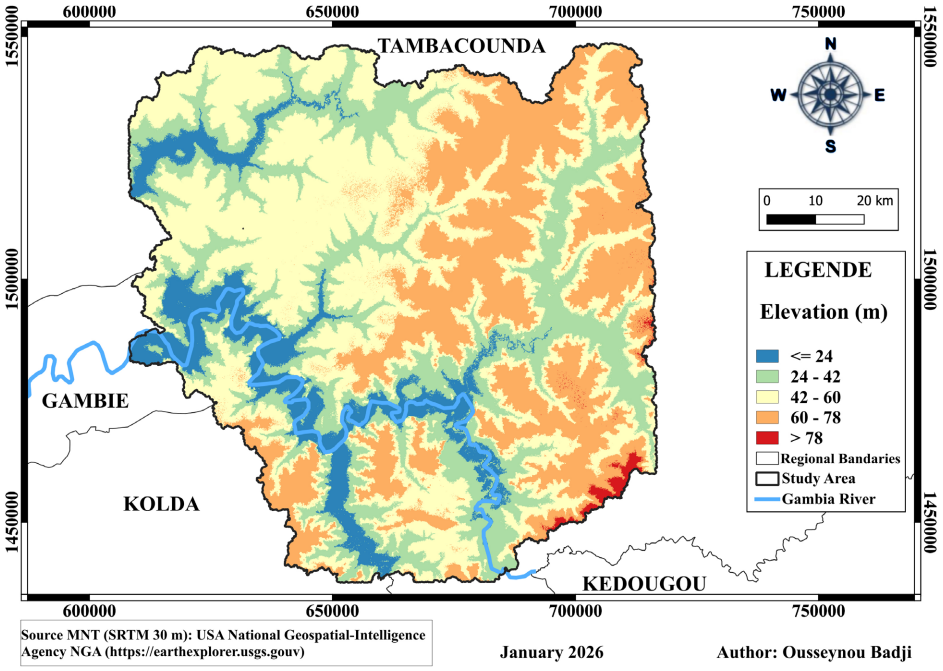

Figure 7. Elevation index (E) in the basin.

sometimes reduce risk when associated with a dense channel network that facilitates water evacuation [32]. Conversely, other studies observe that immediate proximity to watercourses can increase risk [29], illustrating the dual role of this parameter depending on local hydrographic structure. The spatial distribution of proximity to the drainage network is illustrated in **Figure 8**, which presents the distance index (*D*) relative to drainage channels across the basin.

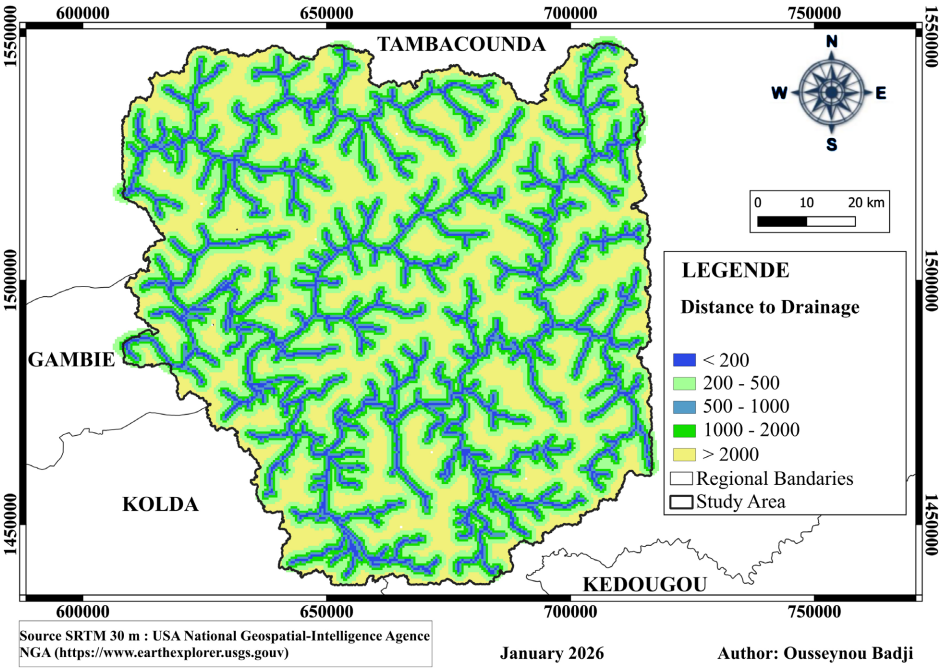

Figure 8. Distance index relative to the drainage network (D) in the basin.

3.2. Spatial Flood Susceptibility Index

The spatial analysis derived from the FIGUSED index reveals a clear structuring of flood susceptibility levels within the study area. The resulting risk classes align with existing literature, where the combination of morphometric and hydrological factors is recognized as a key determinant of vulnerability. Several previous studies have emphasized the importance of these parameters in risk prioritization, particularly in humid and sub-humid tropical environments [8] [15].

Low-risk zones, with index values ranging from 0.5 to 56.6, cover 3810.18 km^2 (39.91% of the territory). These relatively stable areas are located at intermediate elevations or farther from major drainage axes. This distribution is consistent with observations by Danumah *et al.* (2016), who noted that minimally exposed sectors typically occur on moderately elevated topographic units offering favorable conditions for socioeconomic development. Similar findings were reported by Purwanto (2022), who highlighted that areas combining moderate slopes and well-drained soils generally exhibit low flood susceptibility, even in regions affected by intense hydrometeorological dynamics. Thus, the predominance of low-risk areas in the present study follows a spatial logic widely documented in earlier research.

Moderate risk zones (56.6 - 62.8) represent 1905.38 km^2 (19.96% of the total area). These areas correspond to hydromorphological transition zones characterized by gentle slopes and growing proximity to drainage networks. The literature indicates that such intermediate zones are often sensitive to seasonal hydrological variations and require specific management strategies. Nguru *et al.* (2023) argue that implementing retention basins and improved stormwater systems in moderate risk zones significantly reduces recurrent overflow events. The conclusions of Tikuye (2025) also support this idea, demonstrating that hydrologically intermediate areas may experience a rapid increase in sensitivity in the absence of adequate water control infrastructure. These findings indicate that although moderately exposed zones remain usable, they demand cautious and proactive spatial planning.

High risk zones (62.8 - 89.4), representing 3831.34 km^2 (40.12%), are concentrated mostly along riverbeds, depressions, and floodplains. This spatial pattern aligns with findings by Kazakis *et al.* (2015), who showed in the Rhodope–Evros region that low lying terrain near hydrographic networks consistently formed high susceptibility hotspots, accounting for 42% of the analyzed area. Similarly, Husein *et al.* (2025) and Fagunloye (2024) highlight the major influence of drainage density, infiltration capacity, and slope in amplifying flood hazards, especially where human activities increase pressure on natural outlets.

A complementary analysis incorporating the distribution of economic actors mainly GIEs and private companies reveals a significant concentration near river courses. Eight actors are located within 200 m of drainage paths, one between 200 and 500 m, and one between 500 and 1000 m. This pattern echoes the conclusions of Kazakis *et al.* (2015), who demonstrated that infrastructures located within 300 m of drainage channels are highly exposed to direct overflow and soil saturation

processes. It is also consistent with observations from Nguru *et al.* (2023), who note that proximity to hydrological axes represents a major aggravating factor in flood materialization.

Thus, the GIEs located within the 0 - 200 m buffer (e.g., Tilo Tilo, Bassacounda, Yendounane 2) are positioned in the most threatened areas and should be prioritized for structural interventions such as dikes, diversion channels, or rapid evacuation systems. Given the limited financial and technical capacities of most GIEs in the region, low-cost and community-based adaptation measures can significantly reduce exposure. These include: 1) the creation of small earthen diversion channels downstream of plots to redirect excess runoff, 2) routine maintenance of existing drainage ditches, 3) installation of low-cost PVC check-valves to prevent backflow from river channels, and 4) community-level early warning systems relying on SMS alerts triggered by local rainfall thresholds. Additional measures such as mulching, micro-basins or vegetative buffer strips around plantations can further enhance infiltration and reduce surface water stagnation.

Table 4 presents the classes of parameters used in the FIGUSED-S method along with their corresponding values.

Table 4. FIGUSED-S method parameter classes and corresponding values.

Parameters	Classes	Ranking	Area (km²)	Share (%)
F: Flow Accumulation	≤1575165.4000	2	5230.825	54.045
	1575165.4000 - 3150330.8000	4	2494.663	25.770
	3150330.8000 - 4725496.2000	6	1953.070	20.179
	4725496.2000 - 6300661.6000	8	0	0
	>6300661.6000	10	0	0
I: Rainfall Intensity	≤50	2	3743.038	38.670
	50 - 100	4	155.774	1.609
	100 - 150	6	429.272	4.435
	150 - 200	8	2785.367	28.776
	>200	10	2565.794	26.508
G: Geology	Lithosols on lateritic crust	2	3957.393	40.884
	Regosols on gravelly material	4	1108.412	11.451
	Tropical ferruginous soils	6	1414.617	14.615
	Hydromorphic soils	8	277.644	2.868
	Weakly developed soils	10	2474.906	25.569
U: Land Use	Cropland	2	721.1774	7.456
	Gambia River	4	31.5815	0.327
	Settlement	6	57.0283	0.590
	Bare soil	8	6861.2879	70.938
	Vegetation	10	2008.1863	20.762

Continued

S: Slope	≤1.6174	10	1848.660	19.099
	1.6174 - 2.3795	8	2001.392	20.677
	2.3795 - 3.2348	6	1797.503	18.570
	3.2348 - 4.6215	4	2072.774	21.414
	>4.6215	2	1958.989	20.239
E: Elevation	≤24	2	889.721	9.192
	24 - 42	4	2223.902	22.975
	42 - 60	6	3754.574	38.789
	60 - 78	8	2730.572	28.210
	>78	10	80.691	0.834
D: Distance to Drainage	<200	10	848.449	8.699
	200 - 500	8	1185.040	12.150
	501 - 1000	6	1823.044	18.691
	1001 - 2000	4	3135.989	32.153
	>2000	2	2760.905	28.307
FIGUSED: Flood Risk	20.5 - 56.6	Low	3810.18	39.91
	56.6 - 62.8	Moderate	1905.38	19.96
	62.8 - 89.4	High	3831.34	40.12

Tikuye (2025) showed that localized interventions can reduce flooded surfaces by up to 30% during exceptional flood events. Actors located between 200 and 500 m such as Gouloumbou1 and Nguene1 remain exposed to indirect effects such as concentrated runoff or soil saturation. Structures located between 500 and 1000 m face residual risks whose magnitude depends heavily on local morphology and existing infrastructure.

Overall, the spatial distribution of risk levels reveals a relatively balanced representation of low, moderate, and high classes, though with a marked predominance of extreme categories. This pattern supports findings by Purwanto (2022), who noted that territories combining large low risk areas and highly sensitive zones along drainage networks require differentiated management strategies. Consequently, it is essential to tailor structural and non structural measures to each risk category: strengthen heavy protections (dikes, reservoirs, warning systems) in high risk areas; improve adaptive capacities (retention basins, optimized drainage) in moderate risk zones; and ensure secure, sustainable development of economic investments in low risk areas. This differentiated approach consistent with recommendations from Sahelian and Mediterranean literature constitutes a key lever for enhancing territorial resilience to flood hazards.

The overall spatial distribution of flood risk sensitivity, derived from the FIGUSED methodology, is illustrated in **Figure 9**, which presents the flood susceptibility index across the basin.

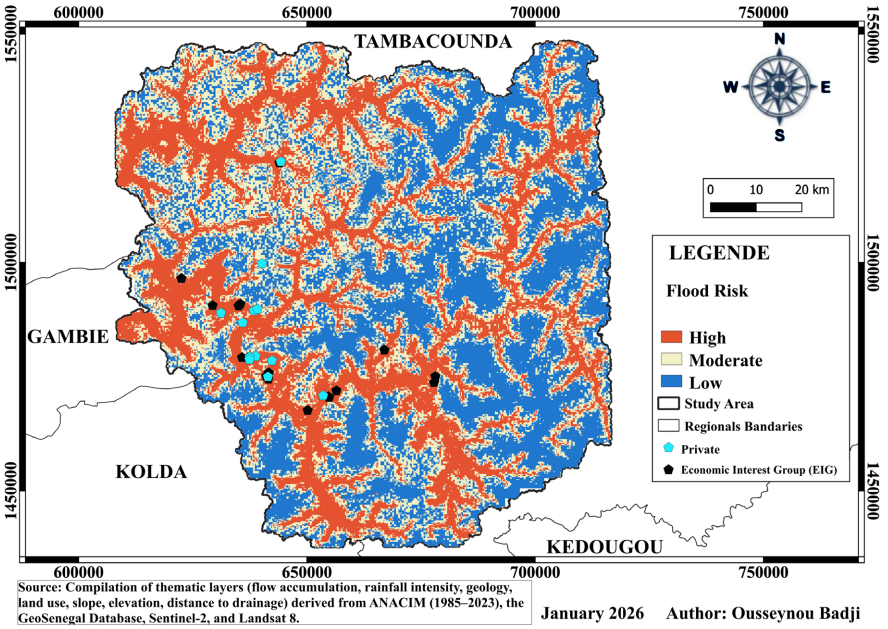

Figure 9. Spatial index of flood risk sensitivity using the FIGUSED methodology.

3.3. Limitations of the FIGUSED-S Method in the Context of the Banana Plantations of Tambacounda

Despite its methodological robustness, the FIGUSED-S approach presents several limitations when applied to the banana-growing areas of Tambacounda. A first limitation lies in the use of the Analytic Hierarchy Process (AHP) for weighting the criteria. As highlighted by Danumah *et al.* (2016), AHP relies on expert judgment, the subjectivity of which may introduce significant biases, particularly in the assessment of the relative influence of topographic, hydrological, or pedological parameters in flood generation. This dependence on expert perception may lead to overestimation or underestimation of key factors such as slope or drainage capacity, a challenge also reported by Husein *et al.* (2025) in their studies on multicriteria flood-risk prioritization.

In addition, the 30-m spatial resolution of the SRTM DEM, widely used within the FIGUSED-S framework, represents another major limitation. Several authors, including Purwanto (2022), note that this resolution is insufficient to capture micro-reliefs and micro-depressions, which are essential features in agricultural systems with fine parcel structure. Such spatial limitations may lead to an underdetection of water-stagnation areas or secondary thalwegs, resulting in a less accurate representation of actual flood sensitivity.

Another critical issue is the essentially static nature of FIGUSED-S. As pointed out by Nguru (2023), multicriteria approaches based on the current state of the landscape do not account for the temporal evolution of key factors such as increasingly intense rainfall, shifts in cultivated areas, or diffuse urbanization, all of which modify runoff patterns. Tikuye (2025) similarly shows that disregarding the spatio-temporal variability of rainfall in static models leads to representations that can quickly become outdated in environments experiencing accelerated climate

change. In Tambacounda, land-use patterns have evolved rapidly over the past decade, with a documented expansion of irrigated banana perimeters toward low-lying hydromorphic areas (Diallo, 2021). Similarly, ANACIM data show an increase in extreme rainfall events since 2018, especially during the 2020, 2022 and 2023 rainy seasons, which resulted in several thousand hectares of cropland being flooded. These recent shifts illustrate the limitations of static models in capturing short-term environmental dynamics.

The FIGUSED-S method also overlooks interactions between surface water and groundwater. Yet, as demonstrated by Kazakis *et al.* (2015), groundwater rise and the interconnection between surface and subsurface systems can significantly amplify flooding, particularly in areas with shallow water tables. This omission may result in an underestimation of saturation-related dynamics, which are frequent in the agricultural plains of Tambacounda.

The agronomic specificities of banana plantations represent another major limitation. Processes such as soil compaction caused by agricultural machinery, internal infrastructures like buried drains or drainage ditches, and intensive cultivation practices are not incorporated into the FIGUSED-S model. However, Fagunloye (2024) underscores that the effectiveness of agricultural drainage systems can substantially alter runoff dynamics and artificially lower the levels of sensitivity identified by conventional approaches.

Finally, the validation of results remains limited. Most comparable studies rely more on historical data than on recent and continuous field observations (Purwanto, 2022; Nguru, 2023). This discrepancy between historical records and current dynamics constitutes a major weakness in regions where environmental and anthropogenic changes are rapid. Without robust ground-truth validation, FIGUSED-S outputs may therefore lack precision, especially in highly modified and rapidly evolving agricultural environments such as the banana plantations of Tambacounda.

These limitations highlight the need for methodological adaptation to improve the relevance of FIGUSED-S in the local context. Integrating higher-resolution data, accounting for temporal variability, and calibrating the model using recent field observations would help produce a more reliable mapping that better reflects the realities of agricultural systems in Tambacounda.

4. Conclusions

The application of the multicriteria FIGUSED method within a GIS environment made it possible to accurately identify the areas most vulnerable to flooding within the banana production zones of Tambacounda. By combining seven key environmental parameters, flow accumulation, slope, elevation, distance to the drainage network, geology, land use, and rainfall, this approach produced a spatially explicit susceptibility map supported by an objective weighting process through the AHP method.

The results show that more than 40% of the study area is exposed to a very high

flood risk, concentrated in the alluvial plains near the Gambia River, where the majority of irrigated plots are also located. Conversely, lower risk zones are found on moderate reliefs, which are less favorable to intensive banana cultivation. The analysis of the distribution of economic actors particularly GIEs and private structures reveals a strong concentration in areas close to the hydrographic network, with several facilities located less than 200 meters from watercourses. This functional proximity increases their exposure to flood hazards, justifying the implementation of targeted protection measures such as dikes, retention basins, and localized alert systems. In contrast, farms located farther away show potential for securing agricultural production, provided that resilient practices are integrated.

This study therefore provides a scientific basis for implementing targeted adaptation strategies, including strengthening drainage systems, reorganizing land parcels located in high-risk zones, and guiding new agricultural developments toward less exposed areas. It also highlights the need to integrate GIS tools and multicriteria indices into public policies for hydrological resilience in Sahelian contexts. Ultimately, the proposed approach could be replicated in other agricultural watersheds exposed to similar hazards, contributing to more sustainable territorial management in the face of climate change.

Conflicts of Interest

The authors declare no conflicts of interest regarding the publication of this paper.

References

[1] Busayo, E.T., Kalumba, A.M., Afuye, G.A., Olusola, A.O., Ololade, O.O. and Orimoloye, I.R. (2022) Rediscovering South Africa: Flood Disaster Risk Management through Ecosystem-Based Adaptation. *Environmental and Sustainability Indicators*, **14**, Article ID: 100175. https://doi.org/10.1016/j.indic.2022.100175

[2] Faye, C., Dièye, S., Fall, A. and Solly, B. (2021) Cartographie des Risques d'Inondation à l'Échelle du Bassin Fluvial à l'Aide de l'Indice de Potentiel d'Inondation: Cas du Sous-Bassin du Niéri-Ko (Bassin de la Gambie). http://rivieresdusud.uasz.sn/xmlui/handle/123456789/1473

[3] Muzamil, S.A.H.B.S., Zainun, N.Y., Ajman, N.N., Sulaiman, N., Khahro, S.H., Rohani, M.M., *et al.* (2022) Proposed Framework for the Flood Disaster Management Cycle in Malaysia. *Sustainability*, **14**, Article 4088. https://doi.org/10.3390/su14074088

[4] Yin, Q., Ntim-Amo, G., Ran, R., Xu, D., Ansah, S., Hu, J., *et al.* (2021) Flood Disaster Risk Perception and Urban Households' Flood Disaster Preparedness: The Case of Accra Metropolis in Ghana. *Water*, **13**, Article 2328. https://doi.org/10.3390/w13172328

[5] Fiorillo, E., Issa, H., Rocchi, L. and Tarchiani, V. (2015). Manuel de la base de données des inondations. Projet Adaptation au Changement Climatique, Prévention des Catastrophes et Développement Agricole pour la Sécurité Alimentaire (ANADIA), Rapport n°5, 37 p. https://www.inondations-niger.org/data/files/MUA_BDINA_V1_2.pdf

[6] Bronfort, S. (2017) Les Stratégies d'Adaptation Face au Risque d'Inondation dans les Zones d'Habitat Spontané de Ouagadougou, Burkina Faso.

https://matheo.uliege.be/bitstream/2268.2/3317/7/Sacha_Bronfort_Memoire_SGE_PED_2016-2017%20(2).pdf

[7] Tanguy, M. (2012) Cartographie du Risque d'Inondation en Milieu Urbain Adaptée à la Gestion de Crise: Analyse Préliminaire. https://espace.inrs.ca/id/eprint/1641/1/R001395.pdf

[8] Danumah, J.H., Odai, S.N., Saley, B.M., Szarzynski, J., Thiel, M., Kwaku, A., *et al.* (2016) Flood Risk Assessment and Mapping in Abidjan District Using Multi-Criteria Analysis (AHP) Model and Geoinformation Techniques, (Cote d'Ivoire). *Geoenvironmental Disasters*, **3**, Article No. 10. https://doi.org/10.1186/s40677-016-0044-y

[9] FAO (2020) Examen du Marché de la Banane: Résultats Préliminaires 2019. https://www.fao.org

[10] Nguru, W., Abera, W., Ouedraogo, I., Chege, C., Kane, B., Bougouma, K., *et al.* (2023) Spatial Estimation of Flood Residual Water Cultivation (FRWC) Potential for Food Security in Sédhiou and Tambacounda Regions of Sénégal. *Agricultural Water Management*, **287**, Article ID: 108445. https://doi.org/10.1016/j.agwat.2023.108445

[11] Fagunloye, O.C. (2024) Mapping of Flood Risk Zones Using Multi-Criteria Approach and Radar a Case Study of Ala and Akure-Ofosu Communities, Ondo State, Nigeria. *International Journal of Geosciences*, **15**, 605-631. https://doi.org/10.4236/ijg.2024.158035

[12] Badji, S. (2017) Le Sud du Sénégal à l'Heure de la Culture Irriguée de la Banane: Innovations Agricoles et Dynamiques Territoriales. Ph.D. Thesis, Université Panthéon-Sorbonne Paris I/Université de Saint-Louis. https://theses.hal.science/tel-01737065/

[13] Diallo, A. (2021) Aménagements Hydro-Agricoles et Gestion de l'Eau dans les Bananeraies de la Zone de Gouloumbou (Tambacounda). https://rivieresdusud.uasz.sn/handle/123456789/1434

[14] Kazakis, N., Kougias, I. and Patsialis, T. (2015) Assessment of Flood Hazard Areas at a Regional Scale Using an Index-Based Approach and Analytical Hierarchy Process: Application in Rhodope-Evros Region, Greece. *Science of the Total Environment*, **538**, 555-563. https://doi.org/10.1016/j.scitotenv.2015.08.055

[15] Purwanto, A., Rustam, R., Andrasmoro, D. and Eviliyanto, E. (2022) Flood Risk Mapping Using GIS and Multi-Criteria Analysis at Nanga Pinoh West Kalimantan Area. *Indonesian Journal of Geography*, **54**, 463-470. https://doi.org/10.22146/ijg.69879

[16] Tehrany, M.S., Pradhan, B. and Jebur, M.N. (2014) Flood Susceptibility Mapping Using a Novel Ensemble Weights-Of-Evidence and Support Vector Machine Models in Gis. *Journal of Hydrology*, **512**, 332-343. https://doi.org/10.1016/j.jhydrol.2014.03.008

[17] Husein, M., Takele, T., Diriba, D. and Karuppannan, S. (2025) Flood Hazard and Risk Assessment Using GIS and Remote Sensing in the Case of Ziway Lake Watershed, Central Main Ethiopian Rift. *Environmental and Sustainability Indicators*, **28**, Article ID: 100920. https://doi.org/10.1016/j.indic.2025.100920

[18] Roy, P.S., Ramachandran, R.M., Paul, O., Thakur, P.K., Ravan, S., Behera, M.D., *et al.* (2022) Anthropogenic Land Use and Land Cover Changes—A Review on Its Environmental Consequences and Climate Change. *Journal of the Indian Society of Remote Sensing*, **50**, 1615-1640. https://doi.org/10.1007/s12524-022-01569-w

[19] Tikuye, B.G., Ray, R.L., Abeysingha, N.S. and Gurau, S. (2025) Integrating Multi-Criteria Decision Analysis and Geospatial Data for Flood Susceptibility Mapping in Texas, USA. *Progress in Disaster Science*, **28**, Article ID: 100462.

[20] Gomis, D.E.R. (2000) Synthèse Hydrologique du Fleuve Gambie en Amont de Gou-

loumbou. Document interne, non publié.

[21] Ouma, Y. and Tateishi, R. (2014) Urban Flood Vulnerability and Risk Mapping Using Integrated Multi-Parametric AHP and GIS: Methodological Overview and Case Study Assessment. *Water*, **6**, 1515-1545. https://doi.org/10.3390/w6061515

[22] Faye, M., Fall, A., Tine, D., Faye, C.S., Faye, B. and Ndiaye, A. (2019) Evolution pluvio-thermique de 1950 a 2013 au senegal oriental: Cas de la region de Tambacounda. *International Journal of Advanced Research*, **7**, 270-287. https://doi.org/10.21474/ijar01/10152

[23] Demek, J. (1972) Manual of Detailed Geomorphological Mapping. Academia, Prague.

[24] Van Zuidam, R.A. (1983) Guide to Geomorphologic Aerial Photographic Interpretation and Mapping. ITC.

[25] Khosravi, K., Pourghasemi, H.R., Chapi, K. and Bahri, M. (2016) Flash Flood Susceptibility Analysis and Its Mapping Using Different Bivariate Models in Iran: A Comparison between Shannon's Entropy, Statistical Index, and Weighting Factor Models. *Environmental Monitoring and Assessment*, **188**, Article No. 656. https://doi.org/10.1007/s10661-016-5665-9

[26] Rahmati, O., Zeinivand, H. and Besharat, M. (2015) Flood Hazard Zoning in Yasooj Region, Iran, Using GIS and Multi-Criteria Decision Analysis. *Geomatics*, *Natural Hazards and Risk*, **7**, 1000-1017. https://doi.org/10.1080/19475705.2015.1045043

[27] Samanta, S., Koloa, C., Kumar Pal, D. and Palsamanta, B. (2016) Flood Risk Analysis in Lower Part of Markham River Based on Multi-Criteria Decision Approach (MCDA). *Hydrology*, **3**, Article 29. https://doi.org/10.3390/hydrology3030029

[28] Guelbeogo, S., Ouedraogo, L. and Ilboudo, S. (2023) Prévision des crues dans le bassin versant du Kou, Burkina Faso. *International Journal of Biological and Chemical Sciences*, **17**, 1131-1146. https://doi.org/10.4314/ijbcs.v17i3.29

[29] Ullah, K. and Zhang, J. (2020) Gis-Based Flood Hazard Mapping Using Relative Frequency Ratio Method: A Case Study of Panjkora River Basin, Eastern Hindu Kush, Pakistan. *PLOS ONE*, **15**, e0229153. https://doi.org/10.1371/journal.pone.0229153

[30] Rincón, D., Khan, U.T. and Armenakis, C. (2018) Flood Risk Mapping Using GIS and Multi-Criteria Analysis: A Greater Toronto Area Case Study. *Geosciences*, **8**, Article 275. https://doi.org/10.3390/geosciences8080275

[31] Weday, M.A., Tabor, K.W. and Gemeda, D.O. (2023) Flood Hazards and Risk Mapping Using Geospatial Technologies in Jimma City, Southwestern Ethiopia. *Heliyon*, **9**, e14617. https://doi.org/10.1016/j.heliyon.2023.e14617

[32] Pallard, B., Castellarin, A. and Montanari, A. (2009) A Look at the Links between Drainage Density and Flood Statistics. *Hydrology and Earth System Sciences*, **13**, 1019-1029. https://doi.org/10.5194/hess-13-1019-2009